

## RECOVERY OF Li, Mn, AND Fe FROM $\text{LiFePO}_4/\text{LiMn}_2\text{O}_4$ MIXED WASTE LITHIUM-ION BATTERY CATHODE MATERIALS

Y.-H. Wang <sup>a</sup>, J.-J. Wu <sup>a,b,\*</sup>, G.-C. Hu <sup>a</sup>, W.-H. Ma <sup>a,b</sup>

<sup>a</sup> Faculty of Metallurgical and Energy Engineering, Kunming University of Science and Technology, Kunming, Yunnan, China

<sup>b</sup> National Engineering Laboratory of Vacuum Metallurgy, Kunming University of Science and Technology, Kunming, Yunnan, China

(Received 21 April 2022; Accepted 20 December 2022)

### Abstract

The recovery of metals from the cathode material or used lithium-ion batteries is of both environmental and economic importance. In this study, stepwise precipitation by acid leaching was used to separate and recover lithium, iron, and manganese from the mixed  $\text{LiFePO}_4/\text{LiMn}_2\text{O}_4$  cathode material. The thermodynamic properties of the lithium, iron, and manganese metal phases, especially the stability range, were analyzed using Eh-pH diagrams. The leaching system with sulfuric acid and hydrogen peroxide released  $\text{Fe}^{3+}$ ,  $\text{Mn}^{2+}$ , and  $\text{Li}^+$  ions from the cathode material.  $\text{Fe}^{3+}$  in the leaching solution was precipitated as  $\text{Fe}(\text{OH})_3$ , and finally recovered as  $\text{Fe}_2\text{O}_3$  after calcination.  $\text{Mn}^{2+}$  in the leaching solution was recovered as  $\text{MnCO}_3$ . The remaining  $\text{Li}^+$ -rich solution was evaporated and crystallized into  $\text{Li}_2\text{CO}_3$ . The purity of the recycled  $\text{MnCO}_3$  and  $\text{Li}_2\text{CO}_3$  met the standard of cathode materials for lithium-ion batteries. XRD and XPS analysis showed that the main phase in the leaching residue was  $\text{FePO}_4$ . This process can be used to separate and recover metals from mixed waste lithium-ion battery cathode materials, and it also provides raw materials for the preparation of lithium-ion battery cathode materials.

**Keywords:** Cathode material; Acid leaching; Thermodynamics; Precipitation; Purity

### 1. Introduction

Lithium-ion batteries have low self-discharge, high energy density, light-weight, and low pollution [1, 2]. They have become the main choice as the power supply of electric vehicles and hybrid electric vehicles. However, the service life of lithium-ion batteries is generally only 5 to 8 years, and many waste batteries end up in landfills after their retirement [3]. If electrode materials and electrolytes in waste lithium-ion batteries enter the environment without treatment, this will lead to the waste of metal resources and the pollution of groundwater resources [4, 5, 6]. Cathode materials can be obtained from decommissioned waste lithium-ion batteries by discharge, disassembly, crushing, and screening [7]. The cathode material contains lithium, manganese, iron, and other metals [8, 9], which can be separated by chemical methods and then recycled. The recovery of metal resources from waste lithium-ion batteries cathode materials can reduce environmental pollution and save metal resources [10].

At present, the recovery of cathode materials from lithium-ion batteries is mainly accomplished by

leaching metals into a solution using organic or inorganic acids, followed by recovering metal ions in the solution [11]. Commonly used inorganic acids include sulfuric acid [12], hydrochloric acid [13], and phosphoric acid [14], while organic acids include citric acid [15], formic acid [16], and oxalic acid [17]. In order to make the leaching process easier and more efficient, Pourbaix plots can be thermodynamically predicted and used to determine the appropriate parameters to be employed in the leaching process [18]. The metal ions in the solution can be recovered by adding a precipitant [19, 20], but the precipitation reactions make it difficult to obtain only the target metal because it will co-precipitate with other metal salts [21]. Numerous studies have been done to recover metals from cathode materials, such as  $\text{LiNi}_x\text{Mn}_y\text{Co}_{1-x-y}\text{O}_2$ ,  $\text{LiFePO}_4$ , and  $\text{LiCoO}_2$  [22, 23, 24]. However, only a single cathode material has been studied. Due to the scarcity of metal resources such as lithium, researchers have begun to study lithium-ion batteries with low-priced metals such as iron, manganese, and aluminum as the cathode [1, 25]. The cathode material is the core of a lithium-ion battery, among which  $\text{LiFe}_x\text{Mn}_{1-x}\text{PO}_4$  combines the

Corresponding author: dragon\_wu213@126.com

<https://doi.org/10.2298/JMMB220918002W>



advantages of  $\text{LiFePO}_4$  and  $\text{LiMn}_2\text{O}_4$  and has become a promising cathode material. Because various types of retired lithium-ion batteries are stored in landfills, it is difficult to guarantee that the cathode material obtained by crushing and screening is a single cathode material. Therefore, it is of great practical importance to study the recovery process of metals in mixed cathode materials.

In this study, an acid leaching-stepwise precipitation process was used to recover lithium, iron, and manganese metals from the mixed cathode material  $\text{LiFePO}_4/\text{LiMn}_2\text{O}_4$ . The focus of this study involved recovering metal ions from the solution in a stepwise manner to prepare high-purity  $\text{Li}_2\text{CO}_3$ ,  $\text{MnCO}_3$ , and other lithium-ion battery precursors to recover and reuse metal resources.

## 2. Experimental

### 2.1. Materials

The reagents and chemicals used in the experiments included sulfuric acid (98 wt.%  $\text{H}_2\text{SO}_4$ ), hydrogen peroxide (30 wt.%  $\text{H}_2\text{O}_2$ ), sodium hydroxide (NaOH), and sodium carbonate ( $\text{Na}_2\text{CO}_3$ ), which were of analytical grade and used without purification. ICP-OES analysis was performed on the mixed cathode material powder  $\text{LiFePO}_4/\text{LiMn}_2\text{O}_4$ , in which the contents of the main elements, Li, Mn, Fe, and C, were 3.13%, 9.06%, 19.43%, and 19.15%, respectively.

### 2.2. Experimental procedure

First, the mixed cathode material powder was leached in a concentration of 1 M sulfuric acid (100 mL), to which hydrogen peroxide solution was slowly added. Then, the beaker was sealed and heated in a constant-temperature magnetically-stirred water bath. After the leaching experiment, the sample was immediately removed for filtration separation. The leaching residue was washed many times during filtration to prevent residues from influencing the metal concentration in the leaching solution. After the leaching residue was dried in a vacuum drying oven,

its components were analyzed and further treated (turned to powder by the agate mortar). Valuable metals (lithium, iron, and manganese) were recovered from the leaching solution. The schematic diagram of the gradual recovery of valuable metals from the mixed cathode material powder is shown in Fig. 1. The stepwise recovery of valuable metals was divided into acid leaching and precipitation processes. A leaching system of sulfuric acid and hydrogen peroxide was used to leach lithium, iron, and manganese metals from the mixed cathode material powder. First,  $\text{Fe}^{3+}$  in the leachate was precipitated by adjusting the pH of the system and was finally recovered as  $\text{Fe}_2\text{O}_3$  after calcination. Next, saturated sodium carbonate solution was added to precipitate  $\text{Mn}^{2+}$  in the leachate as  $\text{MnCO}_3$ . Finally, the pH of the leaching solution was adjusted to evaporate and concentrate  $\text{Li}^+$  and recover it as  $\text{Li}_2\text{CO}_3$ .

To avoid large experimental errors, each group of experiments was repeated three times. The leaching efficiency of the metals is expressed by Eq. (1):

$$\alpha = \frac{D \cdot P}{m \cdot M} \cdot 100\% \quad (1)$$

where  $D$  denotes the mass concentration of lithium, manganese, and iron in the leaching solution (g/L);  $P$  denotes the volume of the leaching solution (L);  $m$  denotes the mass of the reaction raw material (g);  $M$  denotes the content of metals in the raw material (%);  $\alpha$  denotes the leaching efficiency of the metal (%).

Metals were recovered from the leachate by precipitation, and the metal recovery efficiency was reflected by the recovery rate, as expressed by Eq. (2):

$$\beta = \left( 1 - \frac{V_2 \cdot C_2}{V_1 \cdot C_1} \right) \cdot 100\% \quad (2)$$

where  $V_2$  denotes the leachate volume after precipitation (L);  $C_2$  denotes the mass concentration of metals in the leachate after precipitation (g/L);  $V_1$  denotes the volume of leachate before precipitation (L);  $C_1$  denotes the mass concentration of metals in the leachate before precipitation (g/L);  $\beta$  denotes the metal recovery efficiency (%).

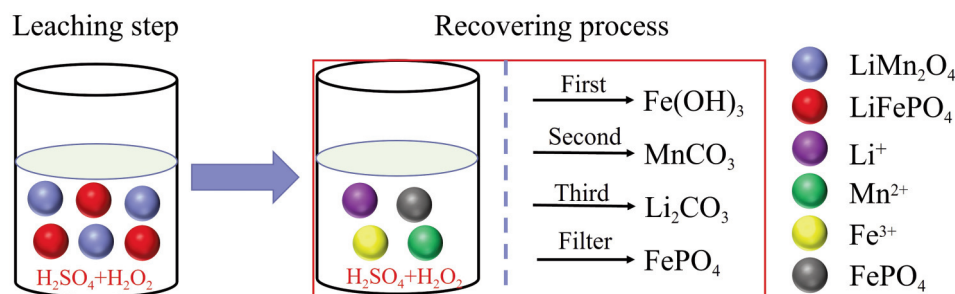


Figure 1. Schematic diagram of step-by-step recovery of valuable metals from mixed cathode materials

Progressive metal recovery causes the loss of other non-target recovered metals, and the loss rate can be expressed by Eq. (3):

$$\gamma = \left(1 - \frac{T_2 \cdot R_2}{T_1 \cdot R_1}\right) \cdot 100\% \quad (3)$$

where  $T_2$  denotes the leachate volume after precipitation (L);  $R_2$  denotes the mass concentration of metal in the leachate after precipitation (g/L);  $T_1$  denotes the volume of leachate before precipitation (L);  $R_1$  denotes the mass concentration of metals in the leachate before precipitation (g/L);  $\gamma$  denotes the metal loss rate (%).

### 2.3. Analysis methods

Field emission scanning electron microscopy (FE-SEM, Nova Nano SEM 450, FEI Company, USA) was used to characterize the morphology of mixed cathode materials, recycled products, and leaching residue. The contents of metal elements in the mixed cathode material and leaching residue, as well as the purity of manganese carbonate and lithium carbonate, were analyzed by inductively coupled plasma atomic emission spectrometry (ICP-OES, 7700x, USA). The mixed cathode materials, recycled products, and leaching residues were characterized by X-ray diffraction (XRD, X'pert3Powder, Netherlands). The surface elements in the leaching residue were analyzed by X-ray photoelectron spectroscopy (XPS, PHI 5000 VersaProbe-II, Japan).

## 3. Results and discussion

### 3.1. Thermodynamic analysis of Fe, Mn, and Li phases

To study the leaching behavior of Li, Fe, and Mn during acid leaching, the thermodynamic characteristics of the different metal phases, especially the stable regions, were analyzed using Eh-pH diagrams in HSC 6.0 software. Fig. 2(a) shows the Eh-pH plot of the Fe-H<sub>2</sub>O system, in which the Fe(III) phase was difficult to dissolve under strongly acidic

conditions until the redox potential reached +0.7704 V. The Fe(II) phase was acid-soluble in this stable region where the redox potential reached the range of -0.4386–0.7704 V and the pH was 6.4697. The leaching conditions in this region were easy to achieve. Because Fe in the cathode material LiFePO<sub>4</sub> existed as Fe(II), it was soluble in sulfuric acid [26]. The Eh-pH diagram of the Mn-H<sub>2</sub>O system in Fig. 2(b) shows that Mn(II) was readily soluble in the acidic region. LiMn<sub>2</sub>O<sub>4</sub> has a spinel structure, in which Mn exists as Mn<sup>3+</sup> and Mn<sup>4+</sup> [27]. Mn(IV) can be dissolved into Mn(II) by forming the intermediate Mn(III) of (Mn<sub>2</sub>O<sub>3</sub>), but this requires strongly acidic or strongly reducing conditions to form a soluble Mn(II) phase. Fig. 2(c) shows the Eh-pH diagram of the Li-C-H<sub>2</sub>O system, which shows that the regions of LiOH and Li<sup>+</sup> phases were partly located within the stable region of water, indicating that Li can be dissolved in both acidic and basic regions. Li<sub>2</sub>CO<sub>3</sub> phase was stable in the alkaline region, which provides theoretical support that the pH of the leachate can be adjusted to recover Li.

### 3.2. Recovery of valuable metals from the leaching solution

#### 3.2.1. Acid leaching

Fig. 3 shows the XRD patterns and SEM images of the mixed raw materials and the corresponding EDS analysis. The XRD analysis of the mixed cathode materials in Fig. 3(c) shows that the main phases of the raw materials were LiFePO<sub>4</sub>, LiMn<sub>2</sub>O<sub>4</sub>, and C (graphite), respectively, and no other impurities were present. As shown in Fig. 3(a), two different shapes of particles were observed: one was lamellar particles, and the other was irregular particles. Combined with the elemental mapping, it can be seen that the lamellar particles were enriched with manganese and oxygen, indicating this was LiMn<sub>2</sub>O<sub>4</sub>. Iron, oxygen, and phosphorus were distributed in the irregular particles, indicating that they were LiFePO<sub>4</sub>. Fig. 3(b) is the EDS analysis, which shows that the mixed raw materials mainly contained iron,

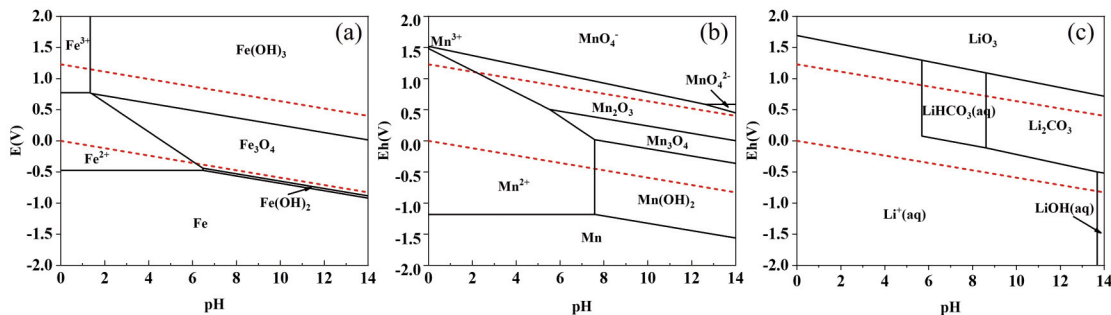
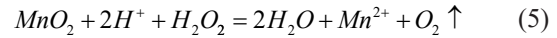
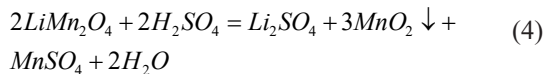


Figure 2. Eh-pH diagram of Fe, Mn and Li leaching system (concentration = 1.0 M at 298 K and 1 atm pressure): (a) Fe-H<sub>2</sub>O; (b) Mn-H<sub>2</sub>O; (c) Li-C-H<sub>2</sub>O



phosphorus, manganese, and a small amount of aluminum, which is the same as the ICP-OES analysis of raw materials. The existence of aluminum was due to the incomplete separation of aluminum foil and the cathode material during crushing and recycling.

The conditions used in this study were as follows: sulfuric acid concentration of 1 M, a solid-liquid ratio of 0.1 g·mL<sup>-1</sup>, hydrogen peroxide volume of 2 mL, leaching time of 30 min, and leaching temperature of 70 °C. Since the purpose of this study was to study the leaching of metals in the cathode materials of mixed waste lithium-ion batteries and the recovery process of metal ions in the leaching solution, this study did not optimize the leaching process parameters. Under the conditions used in the study, the leaching efficiencies of lithium, manganese, and iron in the mixed cathode material were 98.17%, 100%, and 95.90%, respectively. It is very difficult to destroy the Mn-O bonds of LiMn<sub>2</sub>O<sub>4</sub> in the sulfuric acid leaching solution without adding hydrogen peroxide, but the redox reaction can occur (Eq. 4). Lithium was dissolved as Li<sup>+</sup> into the leaching solution, while manganese underwent disproportionation and precipitated as λ-MnO<sub>2</sub>, resulting in a low leaching rate of the leaching system [28]. When hydrogen peroxide was added to the leaching system, MnO<sub>2</sub> was reduced to Mn<sup>2+</sup>, thus diffusing into the solution and improving the leaching efficiency of LiMn<sub>2</sub>O<sub>4</sub> (Eq. 5).



### 3.2.2. Fe<sup>3+</sup> recovery from leachate

The leaching solution obtained by acid leaching contained lithium, manganese, and iron with concentrations of 3.02 g·L<sup>-1</sup>, 8.56 g·L<sup>-1</sup>, and 16.17 g·L<sup>-1</sup>, respectively. There were also large amounts of PO<sub>4</sub><sup>3-</sup>, but Fe<sup>3+</sup> and PO<sub>4</sub><sup>3-</sup> could not form FePO<sub>4</sub> precipitate in the solution due to the low pH of the leaching solution [20]. Lithium, iron, and manganese in the leaching solution precipitated and were recovered in the order of iron, manganese, and lithium by adding precipitant and adjusting the pH. The pH of the leaching solution was adjusted to 5.6 with 2 M NaOH, and Fe<sup>3+</sup> was precipitated by heating and stirring at 80 °C for 1 h. The concentration of Fe<sup>3+</sup> in the leached solution decreased to 0.2 g·L<sup>-1</sup> after purification by precipitation, indicating that 98.8% of Fe<sup>3+</sup> precipitated and was recovered. However, the concentration of lithium and manganese decreased during the precipitation process, which can be explained by the following reasons: (1) The amount of iron precipitate in the solution was large, which consumed the lithium and manganese adsorbed on the precipitation products during solid-liquid separation; (2) the volume of the solution changed before and after leaching. XRD analysis of the precipitation product did not show characteristic peaks, indicating

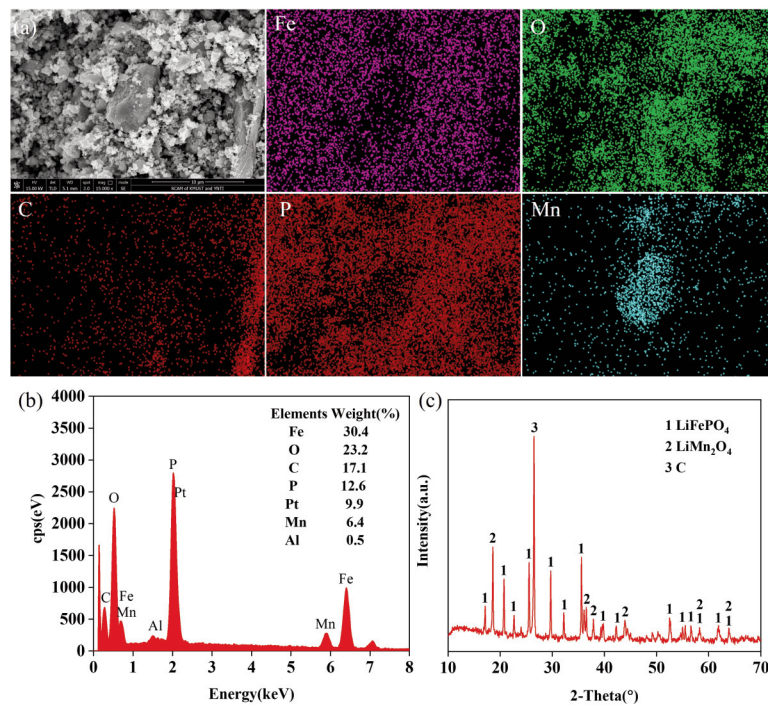


Figure 3. SEM-EDS and XRD analysis of raw materials: (a)-(b) SEM-EDS analysis; (c) XRD spectrum

a poor crystallinity. This may be because  $\text{Fe}^{3+}$  precipitated rapidly under the experimental conditions and formed a flocculent  $\text{Fe}(\text{OH})_3$  precipitate.

To determine its composition, the precipitate was calcined in a muffle furnace at 800 °C for 4 h, and the XRD patterns of the calcined products are shown in Fig. 4. The results indicate that the main phases were  $\text{Fe}_2\text{O}_3$ ,  $\text{MnOOH}$ , and a complex compound of lithium-sodium-manganese-iron. The reasons for the generation of the  $\text{MnOOH}$  phase were analyzed. The mixed cathode material reacted during leaching due to an insufficient amount of hydrogen peroxide (Eq. 4), and then the generated  $\text{MnO}_2$  reacted with  $\text{Mn}^{2+}$  in the leaching solution (Eq. 6) [29]. The existence of lithium-sodium-manganese-iron compounds fully verified that small amounts of sodium, lithium, and manganese in the leaching solution were introduced into the precipitated product after solid-liquid separation. This also explains the lower concentration of lithium and manganese in the solution after iron precipitation.

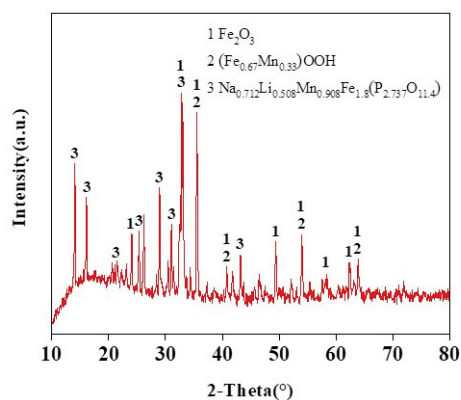
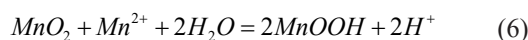


Figure 4. XRD analysis of calcined products

### 3.2.3. $\text{Mn}^{2+}$ recovery from leachate

The leaching solution caused a 34% loss of manganese in the first step of iron precipitation, so the concentration of  $\text{Mn}^{2+}$  in the leaching solution decreased to 3.06 g·L<sup>-1</sup>, which was used for the second step of manganese recovery. First, saturated sodium carbonate solution was added to the filtrate after the purification of  $\text{Fe}^{3+}$ , and then the pH of the solution was controlled to 10.2. Then,  $\text{Mn}^{2+}$  was precipitated by heating and stirring at 80 °C for 9 h. The concentration of the leaching solution after manganese precipitation recovery was reduced to 0.025 g·L<sup>-1</sup>, indicating that the precipitation rate of manganese was 99.3%. Fig. 5(a) shows the XRD pattern of manganese products recovered by precipitation, in which the diffraction characteristic

peaks of the recovered product matched the standard pattern of  $\text{MnCO}_3$  (PDF#83-1763). This indicates that  $\text{Mn}^{2+}$  precipitated in the leaching solution as  $\text{MnCO}_3$ . No obvious impurity peak was found, indicating that the purity of the product was high. In addition, the diffraction peaks of the  $\text{MnCO}_3$  product were sharp, indicating that the product had good crystallinity and a complete cell structure.

Figs. 5(b)-(d) show the SEM-EDS analysis of the recovered manganese carbonate product. From Fig. 5(b), it can be seen that the manganese carbonate particles were spherical, with a particle size of around 1.5 μm. Fig. 5(c) is the EDS analysis of manganese carbonate particles. The element maps of the manganese carbonate particles showed iron and sodium impurities on the surface of the particles. The presence of impurity iron was caused by a very small amount of  $\text{Fe}^{3+}$  that was not completely precipitated in the solution, which produced a manganese carbonate precipitate, as well as unavoidable impurity sodium. The purity of manganese carbonate after ICP-OES analysis was > 96 wt.%, indicating that manganese carbonate can be used to prepare lithium-ion battery cathode materials [30].

### 3.2.4. $\text{Li}^+$ recovery from leachate

After iron and manganese were recovered from the leachate, the remaining solution was lithium-rich, with a concentration of 1.51 g·L<sup>-1</sup>. The pH of the solution was adjusted to 12.0, and then the solution was heated and stirred at 90 °C for 2.5 h. The precipitated lithium was concentrated by evaporation. Fig. 6(a) is the XRD pattern of the recovered lithium products. From Fig. 6(a), it can be seen that the diffraction peaks of recovered lithium products were consistent with the standard spectrum of  $\text{Li}_2\text{CO}_3$  (PDF#80-1307), indicating that lithium in the leaching solution was precipitated as  $\text{Li}_2\text{CO}_3$ . The SEM images of the recovered  $\text{Li}_2\text{CO}_3$  are shown in Fig. 6(b), indicating that the precipitated  $\text{Li}_2\text{CO}_3$  had a cubic shape and aggregated distribution. The mass fraction of the metal was determined by inductively coupled plasma emission spectrometry, and the results showed that  $\text{Li}_2\text{CO}_3$  (purity > 97 wt.%) could be used as a raw material for lithium-ion battery cathode materials [22].

Acid leaching of the mixed waste lithium-ion battery cathode materials was carried out using the sulfuric acid and hydrogen peroxide system. Then, the metal ions in the leachate were subjected to stepwise recovery. The products recovered from the leachate stepwise were  $\text{Fe}(\text{OH})_3$ ,  $\text{MnCO}_3$ , and  $\text{Li}_2\text{CO}_3$ , respectively. Table 1 shows the stepwise recovered metal products from the leaching solution and a summary of the total recovery rate. As can be seen from Table 1, the total recoveries of iron and

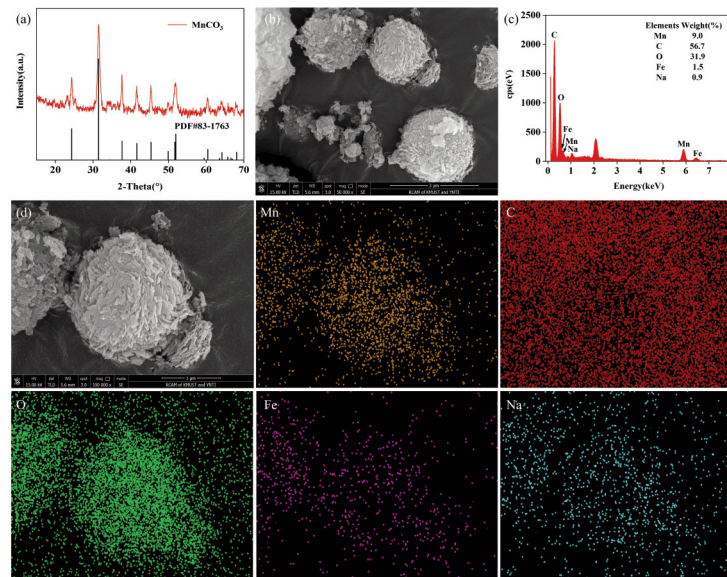


Figure 5. XRD and SEM-EDS analysis of manganese carbonate: (a) XRD spectrum; (b)-(d) SEM-EDS analysis

manganese were 98.8% and 99.95% (including manganese in the form of MnOOH in  $\text{Fe}(\text{OH})_3$ ), respectively, but the percentages of manganese and lithium lost during iron recovery were 65.19% and

### 3.3. Analysis of the leaching residue

$\text{Fe}^{2+}$  in  $\text{LiFePO}_4$  must be oxidized to  $\text{Fe}^{3+}$  to release  $\text{Li}^+$  ions, while high-valent metal ions in  $\text{LiMn}_2\text{O}_4$

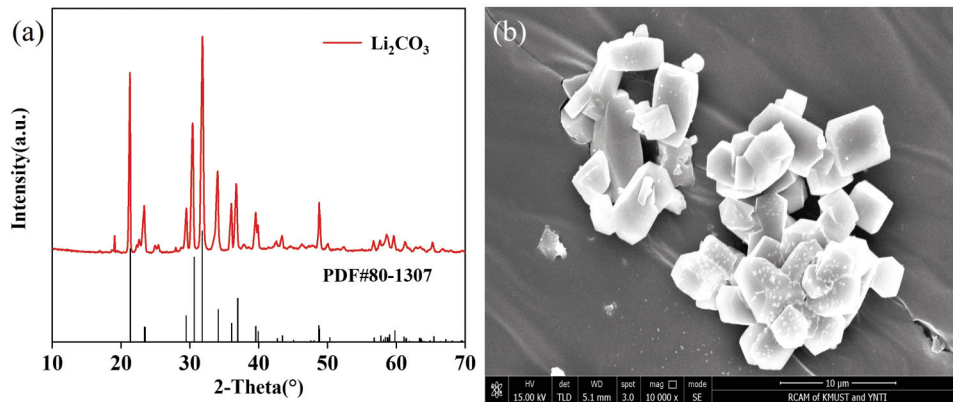


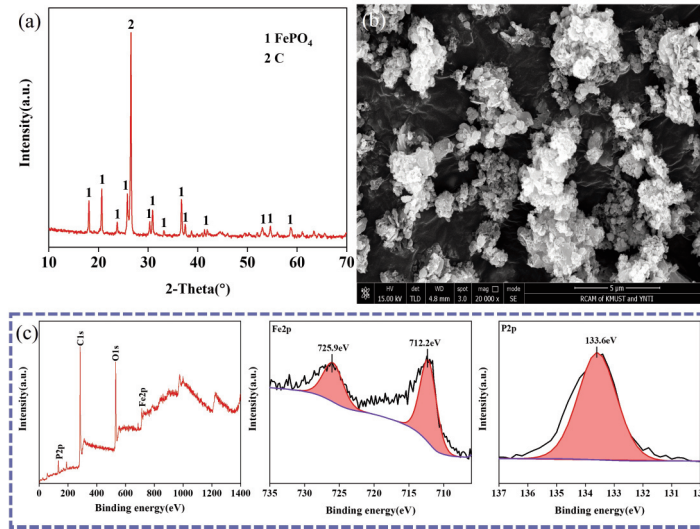
Figure 6. XRD and FE-SEM analysis of lithium carbonate: (a) XRD spectrum; (b) FE-SEM analysis

52.38%, respectively. Therefore, understanding how to reduce the loss of manganese and lithium during iron recovery will be a key step to improving the recovery of valuable metals. All by-products of this process may be valuable input materials for other processes, such as MnOOH, the lithium-sodium-manganese-iron complex compound, and  $\text{Fe}_2\text{O}_3$ . The process recovered iron, manganese, and lithium without generating secondary waste, which is important for recovering metals from used lithium-ion battery cathode materials and has significant economic benefits for environmental and social sustainability.

must be reduced to low-valent  $\text{Mn}^{2+}$  in an acidic solution [31]. The mixed cathode material  $\text{LiFePO}_4/\text{LiMn}_2\text{O}_4$  underwent reactions Eq. (7) and Eq. (8) in the  $\text{H}_2\text{SO}_4\text{-H}_2\text{O}_2$  leaching system. The reaction equation shows that when the leaching system had enough sulfuric acid and hydrogen peroxide,  $\text{LiMn}_2\text{O}_4$  was completely dissolved and mainly existed in the leaching solution as  $\text{Mn}^{2+}$ . Therefore, the residual leaching residue was produced by  $\text{LiFePO}_4$  in the leaching process. Fig. 7 shows the XPS, XRD, and SEM analysis of the leached residue using the  $\text{H}_2\text{SO}_4\text{-H}_2\text{O}_2$  leaching system (particle size:  $D_{50}=9.45\mu\text{m}$ ). Fig. 7(a) shows that the leaching

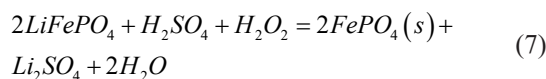
**Table 1.** Summary of results for stepwise metal recovery from leachate

Items	Elements		
	Li	Fe	Mn
Total recovery rate (%)	-	98.8	99.95
Loss rate (%)	52.38	-	65.19
Product forms	Li <sub>2</sub> CO <sub>3</sub>	Fe <sub>2</sub> O <sub>3</sub>	MnCO <sub>3</sub>
Loss forms	Li <sub>2</sub> SO <sub>4</sub>	-	MnOOH/MnSO <sub>4</sub>

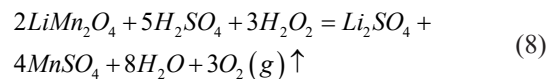
**Figure 7.** XRD, FE-SEM and XPS analysis of leaching residue: (a) XRD spectrum; (b) FE-SEM analysis; (c) XPS analysis

residue was mainly composed of two phases, FePO<sub>4</sub> and impurity C (graphite), without other obvious impurity peaks. Impurity C was removed by calcination. SEM analysis of the leached residue in Fig. 7(b) showed that the morphology of FePO<sub>4</sub> was similar to that of LiFePO<sub>4</sub> in Fig. 3(a) because FePO<sub>4</sub> had an olivine structure similar to that of LiFePO<sub>4</sub> [16]. FePO<sub>4</sub>, which formed after lithium dissociated from LiFePO<sub>4</sub>, can be used to prepare LiFePO<sub>4</sub> cathode material. No manganese-containing phases were detected, and the morphology of LiMn<sub>2</sub>O<sub>4</sub> indicated that LiMn<sub>2</sub>O<sub>4</sub> was completely dissolved, which is consistent with the leaching rate data.

The reaction of LiFePO<sub>4</sub> in H<sub>2</sub>SO<sub>4</sub>-H<sub>2</sub>O<sub>2</sub> leaching system is written as Eq. (7):



The reaction of LiMn<sub>2</sub>O<sub>4</sub> in H<sub>2</sub>SO<sub>4</sub>-H<sub>2</sub>O<sub>2</sub> leaching system is written as Eq. (8):



The elemental composition and chemical states in the leaching residue were measured by XPS. Fig. 7(c) shows that carbon, oxygen, phosphorus, and iron were clearly detected, while manganese was not, which

also shows that LiMn<sub>2</sub>O<sub>4</sub> was completely dissolved. The Fe2p spectrum in Fig. 7(c) showed two obvious peaks at 725.9 eV and 712.2 eV, corresponding to Fe2p<sub>1/2</sub> and Fe2p<sub>3/2</sub> of Fe<sup>3+</sup>, respectively [32]. In the P2p spectrum, the peak at 133.6 eV was due to PO<sub>4</sub><sup>3-</sup>. The XPS results showed that the leaching residue obtained from the mixed cathode material after acid leaching was FePO<sub>4</sub>, which was consistent with the XRD results.

#### 4. Conclusion

In this study, a system composed of sulfuric acid and hydrogen peroxide was used as the leaching agent. Under the experimental conditions of 1M sulfuric acid, 2 mL hydrogen peroxide, a leaching temperature of 70 °C, a leaching time of 30 min, and a solid-liquid ratio of 0.1 g·mL<sup>-1</sup>, the leaching efficiencies of lithium, iron, and manganese were 98.17%, 95.90%, and 100%, respectively. Fe<sup>3+</sup> in the leaching solution was precipitated as Fe(OH)<sub>3</sub> and finally recovered as Fe<sub>2</sub>O<sub>3</sub> after calcination. Mn<sup>2+</sup> in the leaching solution was recovered as MnCO<sub>3</sub>, whose purity was > 96 wt.%, as shown by ICP-OES analysis. The remaining Li<sup>+</sup>-rich solution was evaporated and crystallized into Li<sub>2</sub>CO<sub>3</sub>. The metal products (Fe<sub>2</sub>O<sub>3</sub>, MnCO<sub>3</sub>, and Li<sub>2</sub>CO<sub>3</sub>) can be used as raw materials for

new cathode materials in lithium-ion batteries. This stepwise recycling of metals in the cathode materials of waste lithium-ion batteries can effectively avoid the waste of resources and the pollution of the environment.

### Acknowledgements

*The authors wish to acknowledge the financial support on this research from the Talent Training Program of Yunnan of China (202005AC160041).*

### Author's contributions

*Conceptualization: Y.-H. Wang; methodology: Y.-H. Wang; software: G.-C. Hu; validation: Y.-H. Wang and J.-J. Wu; formal analysis: Y.-H. Wang and J.-J. Wu; resources: J.-J. Wu and W.-H. Ma; writing—original draft preparation: Y.-H. Wang; writing—review and editing: Y.-H. Wang. All authors have read and agreed to the published version of the manuscript.*

### Data Availability Statement

*The raw/processed data required to reproduce these findings cannot be shared at this time as the data also forms part of an ongoing study.*

### Conflict of interest statement

*The authors declare that they have no known competing financial interests or personal relationships that could have appeared to influence the work reported in this paper.*

### References

- [1] X.-L. Zeng, J.-H. Li, Innovative application of ionic liquid to separate Al and cathode materials from spent high-power lithium-ion batteries, *Journal of Hazardous Materials*. 271 (2020) 50–56. <https://doi.org/10.1016/j.jhazmat.2014.02.001>.
- [2] L. Li, X.-X. Zhang, M. Li, R.-J. Chen, F. Wu, K. Amine, J. Lu, The recycling of spent lithium-ion batteries: a review of current processes and technologies, *Electrochemical Energy Reviews*, 1 (2018) 461–482. <https://doi.org/10.1007/s41918-018-0012-1>.
- [3] E. Billy, M. Joulié, R. Laucournet, A. Boulineau, E. De Vito, D. Meyer, Dissolution mechanisms of  $\text{LiNi}_{1/3}\text{Mn}_{1/3}\text{Co}_{1/3}\text{O}_2$  positive electrode material from lithium-ion batteries in acid solution, *ACS Applied Materials & Interfaces*, 10 (2018) 16424–16435. <https://doi.org/10.1021/acsami.8b01352>.
- [4] S.-C. He, Z.-H. Liu, Efficient process for recovery of waste  $\text{LiMn}_2\text{O}_4$  cathode material: Precipitation thermodynamic analysis and separation experiments, *Waste Management*. 113 (2020) 105–117. <https://doi.org/10.1016/j.wasman.2020.05.042>.
- [5] J.-F. Xiao, J. Li, Z.-M. Xu, Challenges to future development of spent lithium ion batteries recovery from environmental and technological perspectives, *Environmental Science & Technology*, 54 (2020) 9–25. <https://doi.org/10.1021/acs.est.9b03725>.
- [6] L.-P. He, S.-Y. Sun, X.-F. Song, J.-G. Yu, Leaching process for recovering valuable metals from the  $\text{LiNi}_{1/3}\text{Co}_{1/3}\text{Mn}_{1/3}\text{O}_2$  cathode of lithium-ion batteries, *Waste Management*. 64 (2017) 171–181. <https://doi.org/10.1016/j.wasman.2017.02.011>.
- [7] Y. Yang, G.-Y. Huang, S.-M. Xu, Y.-H. He, X. Liu, Thermal treatment process for the recovery of valuable metals from spent lithium-ion batteries, *Hydrometallurgy*. 165 (2015) 390–396. <https://doi.org/10.1016/j.hydromet.2015.09.025>.
- [8] J.-H. Li, X.-L. Zeng, A. Stevels, Ecodesign in consumer electronics: Past, Present, and Future, *Critical Reviews in Environmental Science and Technology*. 45 (2015) 840–860. <https://doi.org/10.1080/10643389.2014.900245>.
- [9] J. Sencanski, D. Bajuk-bogdanovic, D. Majstorovic, E. Tchernychova, J. Papan, M. Vujkovic, The synthesis of Li(Co-Mn-Ni) $\text{O}_2$  cathode material from spent-Li ion batteries and the proof of its functionality in aqueous lithium and sodium electrolytic solutions, *Journal of Power Sources*. 342 (2017) 690–703. <https://doi.org/10.1016/j.jpowsour.2016.12.115>.
- [10] C.-W. Liu, J. Lin, H.-B. Cao, Y. Zhang, Z. Sun, Recycling of spent lithium-ion batteries in view of lithium recovery: A critical review, *Journal of Cleaner Production*. 228 (2019) 801–813. <https://doi.org/10.1016/j.jclepro.2019.04.304>.
- [11] J. Kumar, R.R. Neiber, J. Park, R.A. Soomro, G.W. Greene, S.A. Mazari, H.Y. Seo, J.H. Lee, M. Shon, D.W. Chang, K.Y. Cho, Recent progress in sustainable recycling of  $\text{LiFePO}_4$ -type lithium-ion batteries: Strategies for highly selective lithium recovery, *Chemical Engineering Journal*. 431 (2022) 133993. <https://doi.org/10.1016/j.cej.2021.133993>.
- [12] P. Meshram, B.D. Pandey, T.R. Mankhand, Hydrometallurgical processing of spent lithium ion batteries (LIBs) in the presence of a reducing agent with emphasis on kinetics of leaching, *Chemical Engineering Journal*. 281 (2015) 418–427. <https://doi.org/10.1016/j.cej.2015.06.071>.
- [13] M.-M. Wang, C.-C. Zhang, F.-S. Zhang, Recycling of spent lithium-ion battery with polyvinyl chloride by mechanochemical process, *Waste Management*. 67 (2017) 232–239. <https://doi.org/10.1016/j.wasman.2017.05.013>.
- [14] D.-C. Bian, Y.-H. Sun, S. Li, Y. Tian, Z.-H. Yang, X.-M. Fan, W.-X. Zhang, A novel process to recycle spent  $\text{LiFePO}_4$  for synthesizing  $\text{LiFePO}_4/\text{C}$  hierarchical microflowers, *Electrochimica Acta*. 190 (2015) 134–140. <https://doi.org/10.1016/j.electacta.2015.12.114>.
- [15] X.-P. Chen, B.-L. Fan, L.-P. Xu, T. Zhou, J.-R. Kong, An atom-economic process for the recovery of high value-added metals from spent lithium-ion batteries, *Journal of Cleaner Production*. 112 (2015) 3562–3570. <https://doi.org/10.1016/j.jclepro.2015.10.132>.
- [16] H. Mahandra, A. Ghahreman, A sustainable process for selective recovery of lithium as lithium phosphate from spent  $\text{LiFePO}_4$  batteries, *Resources Conservation and Recycling*. 175 (2021) 105883. <https://doi.org/10.1016/j.resconrec.2021.105883>.
- [17] E.-S. Fan, L. Li, X.-X. Zhang, Y.-F. Bian, Q. Xue, J.-W. Wu, F. Wu, R.-J. Chen, Selective recovery of Li and Fe



- from spent lithium-ion batteries by an environmentally friendly mechanochemical approach, *ACS Sustainable Chemistry & Engineering*. 6 (2018) 11029–11035. <https://doi.org/10.1021/acssuschemeng.8b02503>.
- [18] J.A. Barragan, J.R.A. Castro, A.A. Peregrina-Lucano, M. Sanchez-Amaya, E.P. Rivero, E.R. Larios-Duran, Leaching of metals from e-waste: From its thermodynamic analysis and design to its implementation and optimization, *ACS Omega*. 6 (2021) 12063–12071. <https://doi.org/10.1021/acsomega.1c00724>.
- [19] S. Gu, L. Zhang, B.-T. Fu, X.-P. Wang, J.W. Ahn, Feasible route for the recovery of strategic metals from mixed lithium-ion batteries cathode materials by precipitation and carbonation, *Chemical Engineering Journal*. 420 (2020) 127561. <https://doi.org/10.1016/j.cej.2020.127561>.
- [20] W.-B. Lou, Y. Zhang, Y. Zhang, S.-L. Zheng, P. Sun, X.-J. Wang, S. Qiao, J.-Z. Li, Y. Zhang, D.-Y. Liu, M. Wenzel, J.-J. Weigand, A facile way to regenerate  $\text{FePO}_4 \cdot 2\text{H}_2\text{O}$  precursor from spent lithium iron phosphate cathode powder: spontaneous precipitation and phase transformation in an acidic medium, *Journal of Alloys and Compounds*. 856 (2020) 158148. <https://doi.org/10.1016/j.jallcom.2020.158148>.
- [21] X.-H. Zhang, H.-B. Cao, Y.-B. Xie, P.-G. Ning, H.-J. An, H.-X. You, F. Nawaz, A closed-loop process for recycling  $\text{LiNi}_{1/3}\text{Co}_{1/3}\text{Mn}_{1/3}\text{O}_2$  from the cathode scraps of lithium-ion batteries: Process optimization and kinetics analysis, *Separation and Purification Technology*. 150 (2015) 186–195. <https://doi.org/10.1016/j.seppur.2015.07.003>.
- [22] W.-F. Gao, X.-H. Zhang, X.-H. Zheng, X. Lin, H.-B. Cao, Y. Zhi, Z. Sun, Lithium carbonate recovery from cathode scrap of spent lithium-ion battery— A closed-loop process, *Environmental Science & Technology*. 51 (2017) 1662–1669. <https://doi.org/10.1021/acs.est.6b03320>.
- [23] P. Yadav, C.-J. Jie, S. Tan, M. Srinivasan, Recycling of cathode from spent lithium iron phosphate batteries, *Journal of Hazardous Materials*. 399 (2020) 123068. <https://doi.org/10.1016/j.jhazmat.2020.123068>.
- [24] S. Ghasa, A. Farzanegan, M. Gharabaghi, H. Abdollahi, Iron scrap, a sustainable reducing agent for waste lithium ions batteries leaching: An environmentally friendly method to treating waste with waste, *Resources Conservation and Recycling*. 166 (2021) 105348. <https://doi.org/10.1016/j.resconrec.2020.105348>.
- [25] R. Gonçalves, P. Sharma, P. Ram, S. Ferdov, M.M. Silva, C.M. Costa, R. Singhal, R.K. Sharma, S. Lanceros-Mendez, Improved electrochemical performance of  $\text{LiMn}_{1.5}\text{M}_{0.5}\text{O}_4$  (M=Ni, Co, Cu) based cathodes for lithium-ion batteries, *Journal of Alloys and Compounds*. 853 (2021) 157208. <https://doi.org/10.1016/j.jallcom.2020.157208>.
- [26] Y.-H.-Z. Wu, K.-G. Zhou, X.-K. Zhang, C.-H. Peng, Y. Jiang, W. Chen, Aluminum separation by sulfuric acid leaching-solvent extraction from Al-bearing  $\text{LiFePO}_4/\text{C}$  powder for recycling of Fe/P, *Waste Management*. 144 (2022) 303–312. <https://doi.org/10.1016/j.wasman.2022.04.007>.
- [27] X.-L. Zeng, J.-H. Li, N. Singh, Recycling of spent lithium-ion battery: A critical review, *Critical Reviews in Environmental Science and Technology*. 44 (2013) 1129–1165. <https://doi.org/10.1080/10643389.2013.763578>.
- [28] T.-C. Liu, A. Dai, J. Lu, Y.-F. Yuan, Y.-G. Xiao, L. Yu, M. Li, J. Gim, L. Ma, J.-J. Liu, C. Zhan, L.-X. Li, J.-X. Zheng, Y. Ren, T.-P. Wu, R. Shahbazian-yassar, J.-G. Wen, F. Pan, K. Amine, Correlation between manganese dissolution and dynamic phase stability in spinel-based lithium-ion battery, *Nature Communications*. 10 (2019) 1–11. <https://doi.org/10.1038/s41467-019-12626-3>.
- [29] K. Kurniawan, J.C. Lee, J. Kim, H.B. Trinh, S. Kim, Augmenting metal leaching from copper anode slime by sulfuric acid in the presence of manganese (IV) oxide and graphite, *Hydrometallurgy*. 205 (2021) 105745. <https://doi.org/10.1016/j.hydromet.2021.105745>.
- [30] N. Zhao, H.-Q. Fan, M.-C. Zhang, X.-H. Ren, C. Wang, H.-J. Peng, H. Li, X.-B. Jiang, X.-Q. Cao, Facile preparation of Ni-doped  $\text{MnCO}_3$  materials with controlled morphology for high-performance supercapacitor electrodes, *Ceramics International*. 45 (2018) 5266–5275. <https://doi.org/10.1016/j.ceramint.2018.11.224>.
- [31] L. Yao, Y.-B. Xi, H.-J. Han, W.-W. Li, C.-J. Wang, Y. Feng,  $\text{LiMn}_2\text{O}_4$  prepared from waste lithium ion batteries through sol-gel process, *Journal of Alloys and Compounds*. 868 (2021) 159222. <https://doi.org/10.1016/j.jallcom.2021.159222>.
- [32] Z. Li, D.-F. Liu, J.-C. Xiong, L.-H. He, Z.-W. Zhao, D.-Z. Wang, Selective recovery of lithium and iron phosphate/carbon from spent lithium iron phosphate cathode material by anionic membrane slurry electrolysis, *Waste Management*. 107 (2020) 1–8. <https://doi.org/10.1016/j.wasman.2020.03.017>.



## DOBIJANJE Li, Mn, i Fe IZ $\text{LiFePO}_4/\text{LiMn}_2\text{O}_4$ KATODNOG MATERIJALA KORIŠĆENIH LITIJUM-JONSKIH BATERIJA

Y.-H. Wang <sup>a</sup>, J.-J. Wu <sup>a,b,\*</sup>, G.-C. Hu <sup>a</sup>, W.-H. Ma <sup>a,b</sup>

<sup>a</sup> Fakultet za metalurško i energetska inženjerstvo, Univerzitet nauke i tehnologije u Kunmingu, Kunming, Junan, Kina

<sup>b</sup> Nacionalna inženjerska laboratorija za vakuumsku metalurgiju, Univerzitet nauke i tehnologije u Kunmingu, Kunming, Junan, Kina

### Apstrakt

Dobijanje metala iz katodnog materijala korišćenih litijum-jonskih baterija je kako od ekološkog tako i od ekonomskog značaja. U ovoj studiji, postupno luženje kiselim rastvorima je korišćeno da se odvoje i dobiju litijum, gvožđe i mangan iz mešanog katodnog materijala  $\text{LiFePO}_4/\text{LiMn}_2\text{O}_4$ . Termodinamička svojstva metalnih faza litijuma, gvožđa i mangana, posebno opseg stabilnosti, analizirani su korišćenjem E-pH dijagrama. Sistem luženja sa sumpornom kiselinom i vodonik-peroksidom oslobodio je jone  $\text{Fe}^{3+}$ ,  $\text{Mn}^{2+}$  i  $\text{Li}^+$  iz katodnog materijala.  $\text{Fe}^{3+}$  u rastvoru za luženje je istaložen kao  $\text{Fe}(\text{OH})_3$  i konačno dobijen kao  $\text{Fe}_2\text{O}_3$  nakon kalcinacije.  $\text{Mn}^{2+}$  u rastvoru za luženje je izdvojen kao  $\text{MnCO}_3$ . Preostali rastvor bogat  $\text{Li}^+$  je uparen i kristalizovan do  $\text{Li}_2\text{CO}_3$ . Čistoća recikliranog  $\text{MnCO}_3$  i  $\text{Li}_2\text{CO}_3$  zadovoljila je standard katodnih materijala za litijum-jonske baterije. XRD i XPS analize su pokazale da je glavna faza u ostatku luženja  $\text{FePO}_4$ . Ovaj proces se može koristiti za odvajanje i dobijanje metala iz mešovityh otpadnih materijala katodnih litijum-jonskih baterija, a takođe obezbeđuje sirovine za pripremu katodnih materijala litijum-jonskih baterija.

**Ključne reči:** Katodni materijal; Luženje kiselim rastvorima; Termodinamika; Taloženje; Čistoća

